



Evaluating planetesimal bow shocks as sites for chondrule formation

Fred J. CIESLA,^{1*} Lon L. HOOD,² and Stuart J. WEIDENSCHILLING³

¹NASA Ames Research Center, MS 245-3, Moffett Field, California 94035, USA

²Lunar and Planetary Laboratory, University of Arizona, 1629 East University Boulevard, Tucson, Arizona 85721, USA

³Planetary Science Institute, 1700 East Fort Lowell, Tucson, Arizona 85719, USA

*Corresponding author. E-mail: ciesla@cosmic.arc.nasa.gov

(Received 17 November 2003; revision accepted 28 May 2004)

Abstract—We investigate the possible formation of chondrules by planetesimal bow shocks. The formation of such shocks is modeled using a piecewise parabolic method (PPM) code under a variety of conditions. The results of this modeling are used as a guide to study chondrule formation in a one-dimensional, finite shock wave. This model considers a mixture of chondrule-sized particles and micron-sized dust and models the kinetic vaporization of the solids. We found that only planetesimals with a radius of ~ 1000 km and moving at least ~ 8 km/s with respect to the nebular gas can generate shocks that would allow chondrule-sized particles to have peak temperatures and cooling rates that are generally consistent with what has been inferred for chondrules. Planetesimals with smaller radii tend to produce lower peak temperatures and cooling rates that are too high. However, the peak temperatures of chondrules are only matched for low values of chondrule wavelength-averaged emissivity. Very slow cooling ($< \sim 100$ s of K/hr) can only be achieved if the nebular opacity is low, which may result after a significant amount of material has been accreted into objects that are chondrule-sized or larger, or if chondrules formed in regions of the nebula with small dust concentrations. Large shock waves of approximately the same scale as those formed by gravitational instabilities or tidal interactions between the nebula and a young Jupiter do not require this to match the inferred thermal histories of chondrules.

INTRODUCTION

Chondrules are millimeter-sized, silicate spheres that are abundant in most chondritic meteorites. The textures of these objects suggest that they formed before being incorporated into their respective meteorite parent bodies (for a detailed review of our current understanding of chondrules and their formation, see Jones et al. [2000]). The exact method by which these chondrule melts were formed and kept warm as crystals grew has not yet been identified.

Recently, shock waves within the solar nebula have been shown to be capable of explaining the complex thermal histories that have been inferred for chondrules and possibly allow for the formation of other meteoritic components (Iida et al. 2001; Desch and Connolly 2002; Ciesla and Hood 2002; Ciesla et al. 2003). While such work supports the hypothesis that shock waves were the dominant chondrule forming mechanism in the solar nebula, the source of the shocks still remains to be determined. In the studies mentioned above, large scale shock waves ($> 10^5$ km) were modeled, suggesting that shocks due to gravitational instabilities (Boss 2002) or tidal interactions of Jupiter with

the nebula (Bryden et al. 1999; Rafikov 2002) may have been where chondrules formed. Other possible sources are planetesimals, the orbits of which caused them to attain supersonic velocities with respect to the nebular gas (Hood 1998; Weidenschilling et al. 1998). Such velocities could be attained if the planetesimals were in highly eccentric or inclined orbits around the Sun.

While the existence of planetesimals before the formation of the very primitive chondrules (and thus the chondrite parent bodies) seems paradoxical, it may have been possible given the inferred extended lifetime of the nebula before chondrule formation. Amelin et al. (2002) used Pb-Pb dating to show that chondrules formed 2.5 ± 1.2 Myr after the formation of calcium-aluminum-rich inclusions (CAIs), the first objects to have formed in the solar nebula. This time is much longer than the expected time needed to accrete large bodies in a laminar solar nebula ($\sim 10^4$ yr), and possibly long enough to accrete these same bodies in a weakly turbulent nebula (Weidenschilling 1988; Weidenschilling and Cuzzi 1993). In fact, it is possible that this age of chondrules overlapped the global differentiation of the parent body of the HED meteorites, thought to be the 500 km-diameter asteroid

4 Vesta, which must have occurred no later than 4 Myr after CAI formation (Wadhwa and Russell 2000). If this were the case, then it is reasonable to think that other such bodies existed at the same time but were subsequently removed from the asteroid belt (Chambers and Wetherill 2001). This scenario requires further study due to the dependence on unconstrained parameters used in solar nebula and accretion/coagulation models. For the purposes of this study, we assume that chondrule precursors existed in a nebula where bodies up to 1000 km in size had accreted. These precursors could either have been material that had not yet been accreted by planetesimals or material ejected from the collisions of planetesimals.

In addition, this scenario requires Jupiter to have formed fairly rapidly so that it could stir up planetesimals in time to make chondrules. A rapid formation of Jupiter is possible if it formed via the gravitational instability mechanism (e.g., Boss 2002; Mayer et al. 2002). In addition, recent work suggests that the core accretion mechanism for forming Jupiter can work on much shorter timescales (~ 1 Myr) than previously calculated, provided that the core migrated through the nebula over time (Alibert et al. 2004). Thus, having Jupiter present at the time of chondrule formation is possible through either giant planet formation mechanism. Weidenschilling et al. (1998; see also Marzari and Weidenschilling [2002]) found that, in the solar nebula, planetesimals larger than 10 km could get trapped in resonances with Jupiter and attain velocities of 5 km/s or higher with respect to the nebular gas.

Hood (1998) performed hydrodynamic simulations to investigate the characteristics of bow shocks that would be created by such supersonic planetesimals. He found that the shocks created by these planetesimals would be strong enough to melt silicates in a few seconds, which is consistent with how chondrules are thought to have formed, provided that the planetesimals had relative velocities of at least 5.5–7 km/s with respect to the gas. However, no explicit calculations have been carried out to study the cooling histories of the silicate particles heated by these small-scale (< 100 km) shocks.

Hood and Ciesla (2001) found that cooling rates of particles in a relatively small (< 1000 km) shocked region of the nebula that was filled significantly with micron-sized dust particles could be similar to those of chondrules if certain generous assumptions were made. Some of these assumptions were that no relative motion between the chondrule-sized particles and dust particles existed and that all of the particles were initially at the same temperature throughout the region of interest. If a shock wave passed through a region of the nebula with dust ($d = 1 \mu\text{m}$) and chondrules ($d = 1 \text{mm}$), the particles would move through the gas until they lost their velocity with respect to the gas. The stopping distance of a particle is equal to the distance it must travel before encountering a mass of gas equal to itself. This distance is equal to $x_{\text{stop}} = 2\rho/\rho_g d$, where ρ is the mass density of the particle and ρ_g is the mass density of the gas.

For typical values of ρ and ρ_g (1 g/cm^3 and 10^{-9} g/cm^3 respectively), x_{stop} is $\sim 10^9 d$ ($10^8 d$ in shocked gas where the gas density increases by roughly an order of magnitude over the ambient value). Thus, a millimeter-sized chondrule would have a stopping distance three orders of magnitude greater than that of the micron-sized dust particle. Therefore, the assumption that no relative velocity between the two solid particles would exist is not valid until the larger of these distances has been traversed (~ 200 km for typical values). The relative velocity between these particles could cause the chondrules and dust to be at very different temperatures over a large fraction of the region of interest, which was not considered by Hood and Ciesla (2001).

In this paper, the model of Hood (1998) is extended to investigate whether planetesimal bow shocks could have thermally processed silicates in a manner similar to how chondrules are believed to have been processed. In particular, the cooling rates of the silicates are investigated to see if those predicted in the model are consistent with those expected for chondrules. In the next section, we present new simulations of the bow shocks that would be created by supersonic planetesimals and describe the structure of these shock waves in detail. Using these results as a guide, we develop a one-dimensional model to track the heating and cooling of a particle-gas suspension with a mixture of chondrule-sized and micron-sized particles that is overrun with produced shock waves discussed in the Shock Model section. This model allows for the vaporization and recondensation of the silicates. We discuss the results of this modeling in the Results section. In the Discussion section, we discuss what implications this work has for understanding chondrule formation.

PLANETESIMAL BOW SHOCKS

We have used the publicly available Virginia Hydrodynamics-1 code developed by John Blondin and colleagues that solves the equations of gas dynamics using a Lagrangian remap version of the piecewise parabolic method (PPM). The code is based on the methods outlined in Colella and Woodward (1984) and has been used to simulate a variety of astrophysical problems (e.g., Richards and Ratliff 1998). For this work, we used the code to study the flow of gas around a planetesimal of arbitrary size and velocity in the solar nebula. In our runs, the equation of state for the gas is the ideal gas law, where effects such as dissociation and radiation were not considered. Therefore, the gas behaves adiabatically in these simulations.

In our simulations, we used a two-dimensional, 200×200 Cartesian grid with the planetesimal centered in the middle of the grid. The planetesimal was treated as a high-density, low-pressure fluid with no velocity. The surrounding nebular gas was set at a given temperature and pressure and given an initial, arbitrary velocity with respect to the planetesimal. The code was run until a steady state was

formed and the dynamics of the flow were well established. Since a Cartesian grid is used, the calculated flow is essentially equal to that around an infinite cylinder rather than a spherical planetesimal. Since we ignore the expansion of the gas in the z -direction (into and out of the page), the densities presented here may be slightly higher than they would be in the case of a spherical planetesimal. Thus, we may be overestimating the gas density in the vicinity of a planetesimal—an issue we discuss in detail below.

We considered 10 km, 100 km, and 1000 km radii planetesimals with gas velocities of 4 km/s, 6 km/s, and 8 km/s relative to the planetesimal. These velocities were found to be representative of those found in the model runs of Weidenschilling et al. (1998). Significantly higher velocities would require much greater eccentricities or significant inclinations of the planetesimal's orbit (Hood 1998).

An example of one of our runs is shown in Fig. 1, where we consider a 1000 km planetesimal moving through nebular gas at a velocity of 8 km/s (we focus on this velocity because it creates the strongest shocks and, therefore, the greatest amount of heating of solids in the nebula). This velocity would correspond to a planetesimal with an eccentricity of ~ 0.5 at 3 AU, near the maximum value as found by Marzari and Weidenschilling (2002). The gas is assumed to initially be at a density of 10^{-9} g/cm³ and at a temperature of 400 K upstream of the planetesimal (same values used in Hood [1998]), creating a shock of about Mach 4. In this figure, the density of the gas is shown as it flows around the planetesimal (the dense white object in the center). The gas initially flows from left to right at a velocity of 8 km/s until the flow is disturbed by the planetesimal. The modeled smaller planetesimals produced similar shocks that scale with the size of the planetesimal. For example, the 100 km-radius planetesimal produced results similar to that shown in Fig. 1, except the distances on the two axes were smaller by a factor of 10.

The shock front that forms in this scenario is the parabolic discontinuity between the upstream gas and the denser region behind it. For lower velocities of the upstream gas, the curvature of the shock front is not as great. The shape of this shock front is important to consider in studying the processing of particles suspended in the nebula because the strength of the shock wave is determined by the component of the gas velocity that is perpendicular to the shock front. Since the incident gas is moving directly left to right in Fig. 1, the effective velocity with which it passes through the shock front is less than the initial upstream velocity.

Figure 2 shows how the effective velocity of the shock varies with distance from the center of the planetesimal for the different velocities that were considered. Here, the distance from the center of the planetesimal refers to the impact parameter, or distance perpendicular to the initial gas flow from the center of the planetesimal to the point of interest. The effective velocity was found by tracing a trajectory parallel to the velocity of the upstream gas through the shock and finding

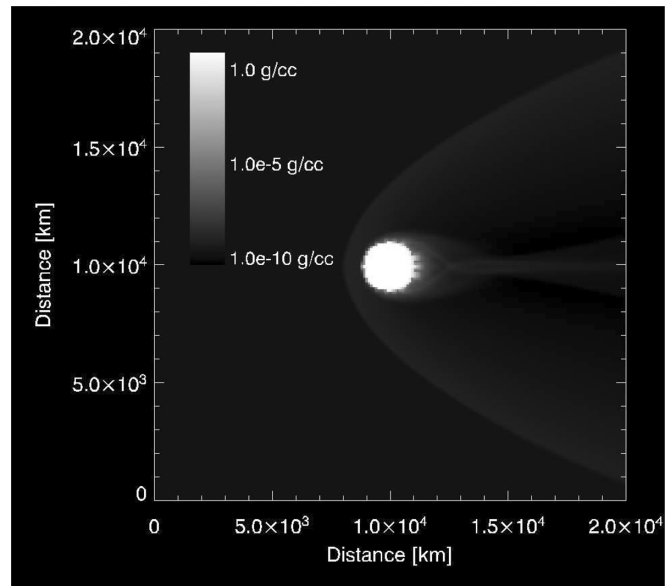


Fig. 1. A simulation of gas flow around a planetesimal using the piecewise parabolic method to solve the equations of flow. The planetesimal is the white object at the center. The density of the gas is shown. The gas is assumed to be owing from the left boundary at 8 km/s at a temperature of 400 K and a density of 10^{-9} g/cm³. The planetesimal is assumed to have a radius of 1000 km.

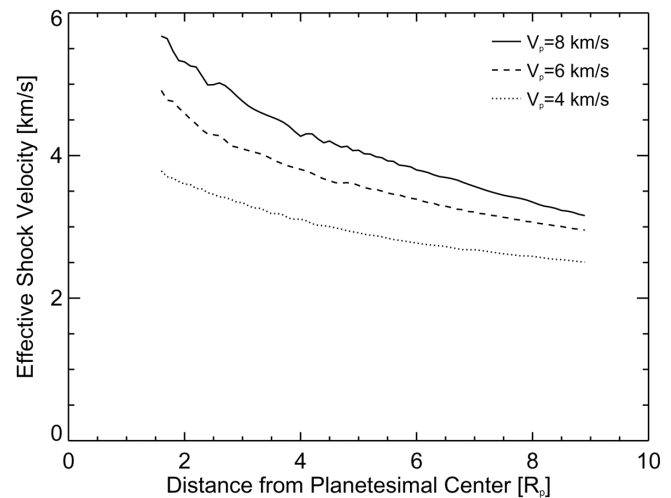


Fig. 2. The effective shock velocities are plotted as a function of distance from the center of the planetesimal for a number of planetesimal-gas relative velocities (V_p). The effective velocity decreases with distance from the planetesimal due to the curvature of the bow shock. The plot is truncated at $\sim 1.5 R_p$ due to the complex flow near the surface of the planetesimal.

the maximum density of the gas along this trajectory. Using the ratio of this maximum density to the density of the upstream gas, we calculated what velocity of shock would be needed to produce that density jump. This treatment determines the shock strength everywhere, accounting for the fact that the gas velocity is not perpendicular to the shock front. Note that the results shown in Fig. 2 are independent of

planetesimal size, as they are plotted in units of planetesimal radii (in the runs of planetesimals of different sizes the results did not vary). The bumps and wiggles of the plot are the result of the finite resolution of the simulations.

The plots are truncated at ~ 1.5 planetesimal radii because the flow of the gas around the surface of the planetesimal is complex and does not allow for simple considerations as those used here. This is because large pressure gradients and lateral flow develop in the gas as it flows around the planetesimal. Particles that enter the bow shock inside of this distance would experience large deflections due to this extreme change in gas flow. Since the region interior to this distance makes up a small volume of space, we feel that neglecting it will not change our results significantly. For the purposes of this study, we focus on the bow shock exterior to 1.5 planetesimal radii where the lateral gas flow is low. We will discuss the likely effects of chondrules entering the shocks inside of this distance at the end of this paper. Overall, it is important to note that the effective shock velocity drops off with increasing distance from the planetesimal and the drop off is steeper with increasing planetesimal velocity.

Figure 3 shows the density profile of the gas along the horizontal trajectory at 1.6 planetesimal radii (1600 km) from the center of the planetesimal in the simulation shown in Fig. 1, where the effective shock velocity is near its maximum value (~ 6 km/s). The distance is measured from the left edge of the simulation. The gas density increases sharply at the shock front, but then slowly decreases with distance. The density actually reaches a value below the original gas density in the wake of the planetesimal (~ 3 planetesimal radii behind the shock) as is found in other simulations of flow around a rigid body. Similar profiles would be found at larger distances from the planetesimal with the maximum density decreasing with increasing distance. Thus, this figure illustrates the structure of the one-dimensional slice of the shock created by the planetesimal and how the gas density (as well as temperature and pressure) is elevated over a finite distance.

SHOCK MODEL

The structure of the shock in the one-dimensional model used here is diagrammed in Fig. 4, where the temperatures of the gas and particles are sketched at different points in the shock. In the region upstream from the shock, particles are heated by the radiation from the hot particles behind the shock front. These particles in turn heat the gas as the shock front approaches. Upon passing through the shock front, the gas properties change as given by the Rankine-Hugoniot relations:

$$\frac{T_2}{T_1} = \frac{[2\gamma M^2 - (\gamma - 1)][(\gamma - 1)M^2 + 2]}{[(\gamma + 1)^2 M^2]} \quad (1)$$

$$\frac{n_2}{n_1} = \frac{(\gamma + 1)M^2}{[(\gamma - 1)M^2 + 2]} \quad (2)$$

$$\frac{v_2}{v_1} = \frac{n_1}{n_2} \quad (3)$$

where T , n , and v represent the gas temperature, number density of gas molecules, and gas velocity with respect to the shock front, and the subscripts 1 and 2 represent the values immediately before and after the shock, respectively, γ is the ratio of specific heats for the gas, and M is the Mach number (the ratio of the speed of the gas with respect to the shock front to the speed of sound in that gas immediately before passage through the front).

Upon passing through the shock front, the gas begins to cool rapidly due to the dissociation of hydrogen molecules. The particles pass through the shock front unaffected and, due to energy and momentum exchange with the gas, are rapidly heated as their velocity with respect to the gas decreases. This rapid heating is what causes the spike in the temperature profile behind the shock front. After reaching their peak temperatures, the particles begin to cool, rapidly at first, before reaching a slower and roughly constant rate (represented by the gentle slope immediately before the end of the shock in the diagram). This slow cooling region is where the radiative energy loss of the particles is only slightly higher than the heat input due to thermal collisions with the gas molecules and the absorbed radiative energy from the surrounding hot particles. This region is called the “relaxation zone” in this model.

After some distance, the gas will start to approach its original, undisturbed, state. This likely happens after the gas expands and cools and the nebula “erases” any evidence of the shock. In our model, upon passing through the end of the shock (assumed to be 3 planetesimal radii behind the shock front), the gas properties return to what they were before crossing through the shock front. The distance of 3 planetesimal radii was chosen to be consistent with Fig. 3 (over this distance, the gas density is at a higher value than in the ambient state). The particles are, again, unaffected when crossing through this region and exchange energy and momentum with the gas as the system relaxes back to its original state (same temperature and velocity as far upstream from the shock). This immersion of the particles back in the cool gas helps quench the particles, causing them to cool very rapidly. In addition, since the gas begins to expand and carry the solids with it, the decrease in concentration of the solids weakens the radiation field that the particles will feel, and thus the solids will not be able to absorb as much energy. Previous shock models that focused on large scale shocks (Iida et al. 2001; Desch and Connolly 2002; Ciesla and Hood 2002; and Ciesla et al. 2003) did not consider what happened to the gas and particles as they exited the relaxation zone of

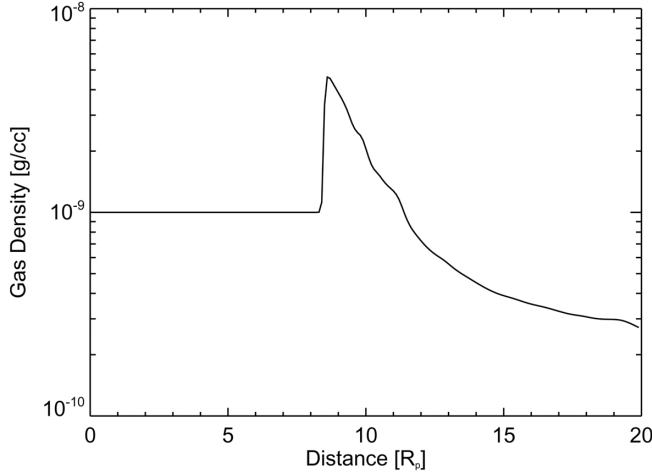


Fig. 3. The gas density is plotted along a horizontal trajectory in Fig. 1 that crosses the bow shock approximately $1.5 R_p$ from the center of the planetesimal. The distance is measured from the left boundary of Fig. 1. The density of the gas decreases immediately behind the shock front, reaching its original, pre-shock value after traveling a distance of approximately $3 R_p$.

the shock. The details likely depend on the source of the shocks, but should be considered in future work.

In treating the system this way, a number of simplifying assumptions have been made. In the simulations described in the Planetesimal Bow Shocks section, the gas properties began to relax back to their pre-shock values as they moved away from the shock front rather than being maintained at the shocked values. In the model used here, the gas expansion is ignored. This means that the gas in the present model is kept at a higher temperature and higher density than would be expected in a real situation. Thus, this allows the gas to transfer a higher amount of energy to the particles (and keep them warm) for a longer period of time. Also, the shocked region is assumed to be infinite in the directions perpendicular to the velocity of the shock for the radiative transfer calculations. Both of these treatments likely lead to underestimating the cooling rates of the particles in our model. These assumptions will be discussed later.

The equations which govern the evolution of the

system are similar to those used by Ciesla and Hood (2002). Along with chondrule-sized particles, we consider the presence of micron-sized dust particles. The dust particles interact with the gas in the same manner as the chondrules. In addition, the chondrules and dust particles are allowed to vaporize as they are heated. This process is handled in the same manner that Moses (1992) treated silicate vaporization. Thus, the equations which govern the evolution of the solids are:

Mass Evolution

$$\frac{dm_{\text{chon}}}{dx} = \frac{1}{v_{\text{chon}}} \frac{dm_{\text{chon}}}{dt} \quad (4)$$

$$\frac{dm_{\text{dust}}}{dx} = \frac{1}{v_{\text{dust}}} \frac{dm_{\text{dust}}}{dt} \quad (5)$$

Density Evolution

$$\frac{d}{dx}(\rho_{\text{chon}} v_{\text{chon}}) = \frac{\rho_{\text{chon}}}{m_{\text{chon}}} v_{\text{chon}} \frac{dm_{\text{chon}}}{dx} \quad (6)$$

$$\frac{d}{dx}(\rho_{\text{dust}} v_{\text{dust}}) = \frac{\rho_{\text{dust}}}{m_{\text{dust}}} v_{\text{dust}} \frac{dm_{\text{dust}}}{dx} \quad (7)$$

Momentum Evolution

$$\frac{d}{dx}(\rho_{\text{chon}} v_{\text{chon}}^2) = F_{D \text{ chon}} + \frac{\rho_{\text{chon}}}{m_{\text{chon}}} v_{\text{chon}}^2 \frac{dm_{\text{chon}}}{dx} \quad (8)$$

$$\frac{d}{dx}(\rho_{\text{dust}} v_{\text{dust}}^2) = F_{D \text{ dust}} + \frac{\rho_{\text{dust}}}{m_{\text{dust}}} v_{\text{dust}}^2 \frac{dm_{\text{dust}}}{dx} \quad (9)$$

Energy Evolution

$$\begin{aligned} \frac{d}{dx} \left[\left(C_{\text{chon}} T_{\text{chon}} + \frac{1}{2} v_{\text{chon}}^2 \right) \rho_{\text{chon}} v_{\text{chon}} \right] &= Q_{g \text{ chon}} + Q_{p \text{ chon}} - Q_{\text{chon rad}} + F_{D \text{ chon}} + L \frac{\rho_{\text{chon}}}{m_{\text{chon}}} v_{\text{chon}} \frac{dm_{\text{chon}}}{dx} + \frac{1}{2} n_{\text{chon}} v_{\text{chon}}^3 \\ &\quad \frac{dm_{\text{chon}}}{dx} + C_{\text{chon}} T_{\text{chon}} \frac{\rho_{\text{chon}}}{m_{\text{chon}}} v_{\text{chon}} \frac{dm_{\text{chon}}}{dx} \end{aligned} \quad (10)$$

$$\begin{aligned} \frac{d}{dx} \left[\left(C_{\text{dust}} T_{\text{dust}} + \frac{1}{2} v_{\text{dust}}^2 \right) \rho_{\text{dust}} v_{\text{dust}} \right] &= Q_{g \text{ dust}} + Q_{p \text{ dust}} - Q_{\text{dust rad}} + F_{D \text{ dust}} + L \frac{\rho_{\text{dust}}}{m_{\text{dust}}} v_{\text{dust}} \frac{dm_{\text{dust}}}{dx} + \frac{1}{2} n_{\text{dust}} v_{\text{dust}}^3 \\ &\quad \frac{dm_{\text{dust}}}{dx} + C_{\text{dust}} T_{\text{dust}} \frac{\rho_{\text{dust}}}{m_{\text{dust}}} v_{\text{dust}} \frac{dm_{\text{dust}}}{dx} \end{aligned} \quad (11)$$

where x is the one-dimensional spatial coordinate, m_{chon} and m_{dust} are the mass of a chondrule and dust particle, v_{chon} and v_{dust} are the velocities of the chondrules and dust particles with respect to the shock front, ρ_{chon} and ρ_{dust} are the mass densities of the chondrules and dust particles suspended in the gas, and T_{chon} and T_{dust} are the temperatures of the chondrules and dust particles. Since we assume that the chondrules and dust particles are composed of the same material, the heat capacities, C_{chon} and C_{dust} , and latent heat of vaporization, L , are assumed to be equal for the two particles. The terms $F_{D\ chon}$ and $F_{D\ dust}$ represent the gas drag force exerted on the particles per unit volume, while $Q_{g\ chon}$ and $Q_{g\ dust}$ represent the rate at which thermal energy is transferred from the gas to the particles per unit volume. These terms are calculated in the same manner as described in Ciesla and Hood (2002). The terms $Q_{p\ chon}$, $Q_{p\ dust}$, $Q_{chon\ rad}$, and $Q_{dust\ rad}$ represent the rate of radiative heating and cooling the particles experience and are calculated using the principles of radiative transfer as described in Desch and Connolly (2002).

The rate at which the particles lose mass is calculated in a manner similar to that employed in Moses (1992). The rate at which the chondrule would lose mass is given by:

$$\frac{dm_{chon}}{dt} = -\pi d_{chon}^2 (P_{eq} - P_{feel}) \left(\frac{\mu}{2\pi k T_{chon}} \right)^{1/2} \quad (12)$$

with a similar equation describing the mass loss for the dust particles. In the equation above, d_{chon} is the diameter of the chondrule, P_{eq} represents the equilibrium vapor pressure of the silicate particles (in dynes/cm²), P_{feel} is the vapor pressure the particles “feel” on their surfaces, μ is the mean molecular mass of the silicate vapor, and k is Boltzmann’s constant (note Moses [1992] assumed that P_{feel} was negligible and, thus, this term was not included in that work). The equilibrium pressure is calculated by:

$$P_{eq} = 10^{A - \frac{B}{T_{chon}}} \quad (13)$$

where $A = 13.176$ and $B = 24,605$ (Moses 1992). The pressure felt by the particle is given by:

$$P_{feel} = n_{SiV} K T_g + \frac{1}{3} \rho_{SiV} (v_{chon} - v_g)^2 \quad (14)$$

where n_{SiV} is the number density of silicate vapor molecules present, ρ_{SiV} is the mass density of those molecules, and v_g is the velocity of the gas with respect to the shock front (Miura et al. 2002). Following Moses (1992), we do not consider the decomposition of the silicate particles into different components (e.g., $Mg_2SiO_4 + 3H_2 \rightarrow 2Mg + SiO + 3H_2O$), but instead treat it as losing a single molecule of mean molecular mass μ . Since chondrules are not pure substances and, therefore would decompose into a number of different species, tracking each species would be difficult. Since the amount of vapor released by vaporization is small compared the amount of hydrogen or helium present, it likely has little effect on the results of this work.

We ignore the effects of collisions between particles in our model and assume that the thermal and dynamical histories of the particles would not be significantly affected by such considerations. Unless collisions would lead to large changes in the size distribution of the particles, which would affect the opacity of the nebula, this assumption should be valid. The most significant outcome of such collisions may be the seeding of chondrule melts by collisions with small dust particles (Connolly and Hewins 1995). This could affect the textures of the chondrule-sized particles processed in these shocks.

The nebular gas also evolves as described by the following equations:

Molecular Hydrogen Evolution

$$\frac{d}{dx} (n_{H_2} v_g) = -\eta_{H_2} \quad (15)$$

Atomic Hydrogen Evolution

$$\frac{d}{dx} (n_H v_g) = 2\eta_{H_2} \quad (16)$$

Helium Evolution

$$\frac{d}{dx} (n_{He} v_g) = 0 \quad (17)$$

Silicate Vapor Evolution

$$\frac{d}{dx} (n_{SiV} v_g) = -\frac{1}{m_{SiV}} \left(\frac{dm_{chon}}{dx} n_{chon} v_{chon} + \frac{dm_{dust}}{dx} n_{dust} v_{dust} \right) \quad (18)$$

Gas Momentum Evolution

$$\frac{d}{dx} (\rho_g v_g^2) + \frac{dP}{dx} = -F_{D\ chon} - F_{D\ dust} - \frac{\rho_{chon}}{m_{chon}} v_{chon}^2 \frac{dm_{chon}}{dx} - \frac{\rho_{dust}}{m_{dust}} v_{dust}^2 \frac{dm_{dust}}{dx} \quad (19)$$

Gas Energy Evolution

$$\frac{d}{dx} \left[\left(e_{H_2} + e_H + e_{He} + e_{SiV} + \frac{1}{2} \rho_g v_g^2 \right) v_g \right] = -Q_{g\ chon} - Q_{g\ dust} - F_{D\ chon} v_{chon} - F_{D\ dust} v_{dust} - Q_{diss} - \frac{1}{2} \frac{\rho_{chon}}{m_{chon}} v_{chon}^3 \frac{dm_{chon}}{dx} - \frac{1}{2} \frac{\rho_{dust}}{m_{dust}} v_{dust}^3 \frac{dm_{dust}}{dx} - C_{p\ chon}^{SiV} \frac{\rho_{chon}}{m_{chon}} v_{chon} \frac{dm_{chon}}{dx} - C_{p\ dust}^{SiV} \frac{\rho_{dust}}{m_{dust}} v_{dust} \frac{dm_{dust}}{dx} \quad (20)$$

where η_{H_2} is the rate of dissociation per unit volume of hydrogen molecules, Q_{diss} is the rate of energy loss due to dissociation per unit volume both calculated as described in Iida et al. (2001), n_{H_2} and n_H are the number densities of hydrogen molecules and atoms, n_{He} is the number density of helium atoms, and ρ_g is the mass density of the nebular gas. The terms e_{H_2} , e_H , e_{He} , and e_{SiV} represent the internal energies of the hydrogen molecules, atoms, and silicate vapor, respectively. They can be calculated using:

$$e_i = \rho_i C_p^i T_g \quad (21)$$

where $i = H_2, H, He,$ or SiV , C_p^i is the specific heat at constant pressure for the corresponding species, and ρ_i is the corresponding mass density.

In this model, we neglect line emission cooling of the nebular gas. This effect has been considered in some shock wave models for chondrule formation (Iida et al. 2001). The importance of this cooling is strongly dependent on the amount of coolant molecules present in the gas, with H_2O being the dominant cooling species. The concentration of water in the nebular gas in the asteroid belt region (where we are assuming chondrules formed) likely varied significantly over time. J. Cuzzi (personal communication) has shown that if there were a major “planetesimal sink” which accreted the solids around it, such as a young Jupiter or a Jovian core near the snow line, the region of the nebula interior to this sink would be depleted in water by diffusion on timescales on the order of $\sim 10^{5-6}$ yr.

The model investigated here requires that Jupiter had grown to significant mass such that the planetesimals near orbital resonances with the planet could be stirred up to supersonic speeds. The results of Amelin et al. (2002) suggest that chondrules formed ~ 2.5 Myr after the formation of the solar nebula. If Jupiter formed over this time (by either core accretion or gravitational instability), then this provides more than enough time for diffusion to remove water from the nebular gas (Stevenson and Lunine 1988; Cyr et al. 1998). In fact, if Jupiter formed by core accretion, the removal of water from the inner nebula may have been required to form the core (Stevenson and Lunine 1988). Thus, neglecting the cooling by line emission from water molecules would be a valid approximation.

If water vapor was not diffusively removed from the inner nebula before the stage of nebula evolution considered here, then it may have played a role in cooling the gas behind the shock waves as discussed by Iida et al. (2001). The main

effect would be causing the gas to cool more quickly, which would also increase the gas density slightly. This likely would cause the particles to reach slightly higher peak temperatures (due to the increase in gas density and, thus, in gas drag heating immediately behind the shock front) but would also likely increase the cooling rates of the particles due to loss of thermal energy to the gas.

For the cases presented, the nebula is assumed to be originally at some temperature, T_i , far upstream of the shock, which sets the forward boundary condition for the radiative transfer calculations. Far behind the shock (thousands of kilometers, determined by the integration), the suspension returns to this same original temperature and, therefore, the end boundary condition for the radiative transfer is the same. In solving the equations that describe the evolution of the system, the temperature of the chondrules is initially calculated after they pass through the shock front based on the other modes of heat transfer. The calculations are then repeated, and the heat transferred due to radiation from the other particles is found using the previously calculated temperature profile as a function of distance. The procedure is repeated until the temperature of the chondrules does not change by more than 1 K.

RESULTS

In all cases presented here, the region of the nebula under consideration has an initial temperature of 400 K, a hydrogen molecule number density of 2.5×10^{14} cm³, and a helium number density of 5×10^{13} cm³ ($\rho_g = 10^{-9}$ g/cm³), for a total pressure of $\sim 10^{-5}$ bars. This gas density is roughly equal to that expected at 2.5 AU in a minimum mass solar nebula, the type used in previous studies of planetesimal bow shocks (Hood 1998; Weidenschilling et al. 1998). The properties of the chondrule-sized particles are the same as those used in Ciesla et al. (2003) (unless otherwise specified): diameter of 0.1 cm, mass density of 3.3 g/cm³, a wavelength averaged emissivity of 0.9, a heat capacity of 10^7 erg g⁻¹ K⁻¹, and a latent heat of melting of 4.5×10^9 erg g⁻¹ spread over the temperature range 1400–1900 K to account for incongruent melting of chondrules. The latent heat of vaporization was assumed to be 10^{11} erg g⁻¹ close to the values used by Moses (1992) and Miura et al. (2002). The dust particles are assumed to have the same properties as the chondrules, due to their assumed similar composition, except they are originally treated as spheres 1 μ m in diameter and have an assumed (constant)

wavelength averaged emissivity of 0.1. This lower emissivity is used to account for the difficulty that small particles have radiating away energy in wavelengths that are large compared to the size of the particle. We assume that the silicate vapor has a mean molecular mass of $50 m_H$ and a specific heat capacity at constant pressure of $9k/2m_{SiV}$, while the values for the hydrogen molecules and atoms are $7k/2m_{H_2}$ and $5k/2m_H$, respectively, and the value for helium is $5k/2m_{He}$.

The dust was considered to have totally vaporized if its mass dropped below $0.001 m_{dust 0}$, where $m_{dust 0}$ is the original mass of a dust particle. In none of the cases presented below did the dust completely vaporize, despite reaching temperatures over 2000 K. This is because as the dust began to lose mass, the particles were cooled due to latent heat effects. Stronger shocks (effective velocity >8 km/s) may have provided enough energy to totally vaporize the particles.

The solids in the model are suspended at a solar ratio with respect to the nebular gas such that $(\rho_{chond} + \rho_{dust})/\rho_g = 0.005$. The mass of the solids is distributed such that 75% of the mass is in chondrule-sized particles and 25% as micron-sized dust (Desch and Connolly 2002). We investigate other possible ratios of chondrules to dust and non-solar solids to gas mass ratios in the section titled Various Chondrules: Dust and Solid-Gas Mass Ratios. The solar values give a chondrule number density of $2.5 \times 10^{-8} \text{ cm}^{-3}$ and a dust number density of 0.85 cm^{-3} .

10-km Planetesimal

The top panel in Fig. 5 shows the temperature evolution of the chondrules with time as they are encountered by a 6 km/s, one-dimensional shock that is 30 km in width, where the width is defined as the distance between the shock front and the shock end (Fig. 4). Time is measured from the time in which the shock front encounters the chondrules. The chondrules are heated by radiation as they approach the shock front, reaching a temperature of ~ 800 K before crossing the shock front. The chondrules then reach a peak temperature of ~ 1440 K before cooling rapidly ($>10^5$ K/hr) below the solidus. The cooling rate of the chondrules while they are above their assumed solidus (1400 K) is shown in the bottom panel of Fig. 5.

It is generally thought that chondrules formed by being heated to temperatures between 1700–2100 K and then cooling during crystallization (temperatures above the solidus) at rates below 1000 K/hr, with some chondrules possibly needing to cool at rates below 100 K/hr at these temperatures (Jones et al. 2000). It has been suggested by some authors that more rapid cooling could also lead to chondrule formation—we return to this issue later in this study. The relatively low peak temperature (<1450 K) and very rapid cooling ($>10^5$ K/hr) of the particles in this simulation do not match those generally inferred for chondrules.

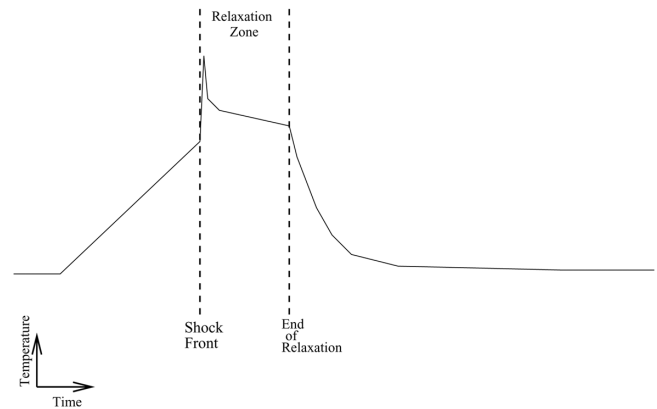


Fig. 4. An approximate thermal profile of the particles (gas) is diagrammed using the shock model. The particles are heated by radiation that leaks out from the shock front as the shock approaches (shock moves from right to left in this figure). Upon passing through the shock front, the particles are heated rapidly by gas drag before cooling as they lose their velocity with respect to the gas. The particles then cool, rapidly at first, and if the shock is wide enough the cooling rate decreases when the particles radiate away slightly more energy than they absorb from the ambient radiation field. Upon passing through the end of the shock, the particles are immersed in gas, the properties of which are identical to what they were immediately upstream of the shock front. The particles then cool very rapidly due to being quenched in cold gas and a weaker radiation field.

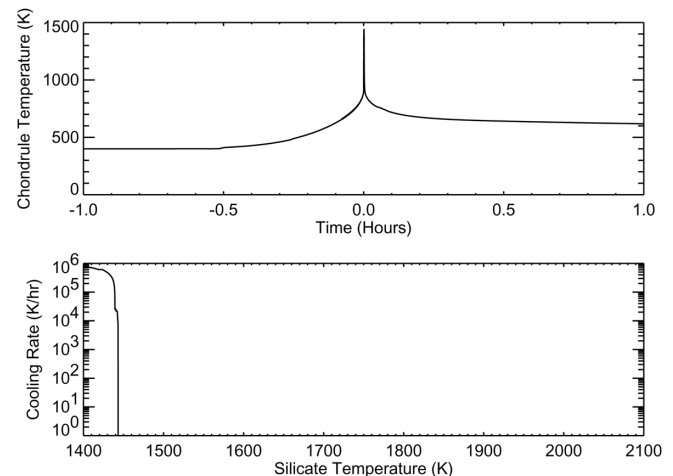


Fig. 5. The top panel shows the temperature evolution of a chondrule-sized particle that encounters a one-dimensional, 30-km-wide shock moving at 6 km/s. The bottom panel shows the cooling rate of the same particle at temperatures above the assumed solidus (1400 K). The cooling rate is zero at the peak temperature of the chondrule but quickly increases to much higher rates.

100-km Planetesimal

The panels in Fig. 6 show the same thermal evolution as described above, except in this case the shock width is 300 km. The solids are again heated by radiation upstream of the shock, this time with the chondrules reaching a

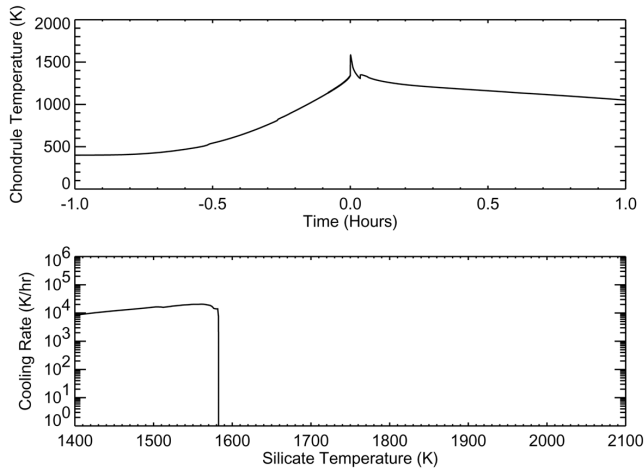


Fig. 6. Same as Fig. 5, except the shock is 300 km wide. The slight increase in temperature after the rapid cooling in the top panel is where the particle passes through the end of the shock and is immersed in the cool but fast moving gas of the nebula. The increase in the particle's temperature is due to the collisions with the fast moving gas. Again, the cooling rate is nearly zero at the peak temperature of the chondrule, but quickly increases to $>10^4$ K/hr before slowly decreasing at lower temperatures.

temperature of ~ 1300 K before crossing the shock front. This higher temperature is due to the fact that the radiation emitted from behind the shock front is more intense due to the larger volume of hot particles within the shock.

The increased width of the shock also allows the chondrules to reach a higher peak temperature (~ 1580 K) than in the case previously considered. This is because the stopping distance of the chondrules (~ 200 km) is less than the width of the shock, and thus they are heated by gas drag over this distance and subjected to a higher radiation field. Since the chondrules completely lose their velocity with respect to the gas, they begin to cool while still within the shocked gas. The higher temperature and density of the gas in this region allow more heat to be transferred to the chondrules through thermal collisions, and therefore they cool at a slower rate than in the previous case.

Upon exiting the shocked region, the particles are moving at a velocity with respect to the shock front that is much less than when they entered the shock region. The gas, as it exits the shock front, returns to the high value it had right before entering the shock front (due to the assumptions made in this model), and therefore there is a relative velocity between it and the chondrules. This causes the chondrules to be heated somewhat, which can be seen as the little rise in temperature after the chondrules have cooled rapidly and before the more gradual cooling begins (~ 0.05 hr after crossing the shock front).

As in the previous case, the predicted peak temperature (<1600 K) in this simulation and the cooling rates ($>10^4$ K/hr) do not match those generally expected for chondrules.

1000-km Planetesimal

The top panel in Fig. 7 shows the temperature evolution of the chondrules in the same situations described, except that the shock is 3000 km in width. The chondrules are heated to an even higher temperature (~ 1400 K) upstream of the shock front due to the larger volume of hot particles leading to a more intense radiation field. This larger volume again helps the chondrules reach a higher peak temperature than in the previous cases.

The cooling of the particles in this case (bottom panel in Fig. 7) is substantially slower than in the cases previously considered. In fact, as the temperature of the chondrules approaches the solidus, the cooling rate is $\sim 10^3$ K/hr, which is the upper limit of expected chondrule cooling rates. Thus, a shock of this size and strength seems to allow for cooling rates comparable to the cooling rates that chondrules are thought to have experienced. While the peak temperature of the chondrules is only ~ 1600 K, it is not far off from temperatures that chondrules are thought to have reached.

In Fig. 8, we show a similar model run as just described, except that the chondrule averaged emissivity is assumed to be 0.1 (as opposed to 0.9). In this case, the chondrules reach a significantly higher peak temperature (~ 2020 K) due to the fact that the chondrules cannot radiate as much energy away during the initial period of heating by gas drag. The particles then cool, rapidly at first, before again reaching a cooling rate of $\sim 10^3$ K/hr as the temperature approaches the solidus. The cooling rate is not greatly affected by the change in chondrule emissivity. Since the emissivity was assumed to be 0.1, the absorptivity was also assumed to be 0.1 to be consistent with Kirchoff's law. Thus, the amount of radiation emitted by the chondrules decreases by the same factor as the amount absorbed (the radiation field is dominated by the dust particles). The interaction between the gas and the dust control how quickly the system cools, and therefore a change in the emissivity has little effect on the cooling of the chondrules. The dust will determine the cooling rate of the system as long as it is the major source of opacity. If the dust were to be completely vaporized (which was not the case in any of our runs), the cooling rate would likely be much lower. This would require the shocks to have greater velocities than considered here.

Various Chondrules:Dust and Solid:Gas Mass Ratios

The ratio of solids to gas in a given location of the nebula may have varied greatly due to the settling of material into a layer at the midplane or due to the accretion of large planetesimals. Similarly, the size distribution of solids may have varied due to the level of turbulence in the nebula, the details of the accretion process, and the location where chondrule formation took place. Thus, we also considered a number of cases where these ratios were different from those

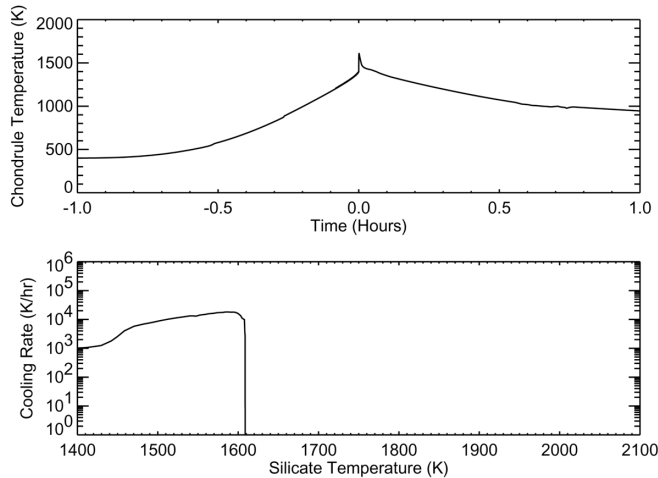


Fig. 7. Same as Fig. 5, except the shock is 3000 km wide. The cooling rate near the solidus is approximately consistent with the fastest cooling rates inferred for chondrules though the peak temperature is slightly below what has been inferred.

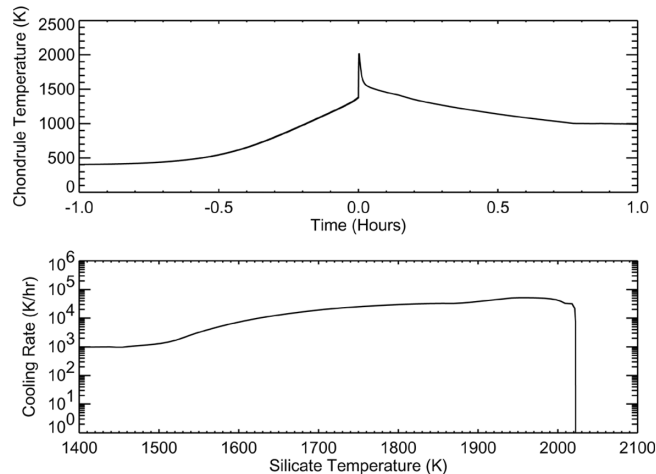


Fig. 8. Same as Fig. 7, except that the particle is assumed to have a much lower wavelength-averaged emissivity. This prevents the particle from radiating as much energy as it is heated by gas drag immediately behind the shock front, and therefore it reaches a higher peak temperature. The particle then cools at a cooling rate of ~ 1000 K/hr, which is consistent with what has been inferred for some chondrules.

described above. All other conditions are the same as described for the 1000 km-radius planetesimal case described above. The results of some of these cases are qualitatively described below.

We considered one case where the distribution of chondrule mass to dust mass was 50:50. The cooling rates of the chondrule-sized particles were found to be much higher than in the cases described previously. This was due to the fact that as the chondrules drift away from the shock front, the optical depth between them and the hot dust immediately behind the shock front increases more rapidly than in the

previous cases. While they are heated initially by drag, the heating due to radiation rapidly decreases. This loss of heating becomes significant as the chondrules are surrounded by cooler (compared to the temperature behind the shock front) dust particles, which still heat the chondrules but to a much lesser extent.

The opposite was true for the case in which the chondrule to dust mass ratio was 90:10. Due to the decrease in opacity, the chondrules are exposed to the radiation from the hot particles immediately behind the shock front for a longer period of time. This helps keep the chondrules from cooling too rapidly so the cooling rate is as low as ~ 10 K/hr. The cooling rate increased rapidly (to ~ 100 K/hr) as the chondrules drifted toward the end of the shock where their radiation is not “trapped” any longer and escapes to the unshocked regions of the nebula.

A similar result was found when we considered cases in which the mass ratio of solids to gas suspended in the nebula was not at the solar value. For those cases that resulted in significant increases in the opacity of the nebula (larger values of fine-grained dust), the cooling rates of the chondrules increased. This is due to the fact that as the chondrules drifted through the shocked gas, the optical depth between them and the hot chondrules immediately behind the shock front increased at a greater rate. Because of this, the chondrules would be shielded from a major heat source, and therefore cool at a greater rate. For cases when the opacity of the nebula decreased (either due to vaporization of fine-grained dust or its depletion due to accretion), the radiation from the hot particles was able to travel further and help keep the chondrules warm for longer periods of time. This correlation of slower cooling rates and lower opacity of the solids was also found in Desch and Connolly (2002) and Ciesla and Hood (2002).

In summary, if chondrule-sized particles had emissivities significantly less than 0.9 (Desch and Connolly [2002] suggest a value of 0.8, which decreases when the chondrules are near their peak temperatures), which may be possible given the uncertainties of the measured optical constants, both the peak temperature and cooling rates could be consistent with what has been inferred for chondrules if they were heated in a 3000 km-wide shock of the type described here. However, cooling rates of 10–100 K/hr, which most chondrules may have experienced (Jones et al. 2000), can be reached only if the amount of dust present in the nebula is small or if much of it is vaporized upon passing through the shock front.

DISCUSSION

In all but one of the cases presented here, the cooling rates and peak temperatures of the particles were not consistent with what has been generally inferred for chondrules. It has been argued that chondrules could have formed by multiple instances of low level heating (peak

temperatures <1700 K) followed by rapid cooling (cooling rates of about a few thousands of K/hr and higher) (Wasson 1996; Wasson and Rubin 2003). If this type of thermal processing did result in textures and chemical zoning similar to those of chondrules, then planetesimal bow shocks could be possible sites for chondrule formation. Experiments investigating these rapid cooling rates are needed.

There was one case presented in which the calculated peak temperature and cooling rate of the silicates matched those inferred for chondrules: the case of a 1000 km planetesimal with low wavelength-averaged emissivities for the chondrule-sized particles. In other cases we studied, the cooling rates in our runs were found to decrease as the amount of dust present decreased. Thus, it is possible that shocks formed by large planetesimals could form chondrules if there were only a small amount of material present as fine-grained dust. However, it is unclear how such a scenario may be achieved in the nebula. One possibility is that the larger particles (millimeter-sized) could settle to the midplane much faster than the dust particles. This would be possible over long periods of time if nebula turbulence works such that only very small ($\ll 1$ mm) particles are prevented from settling to the midplane. This would be possible if the turbulent velocity ($\alpha^{1/2}c_s$, where α is the turbulence parameter and c_s is the local speed of sound) is greater than the settling velocity of the fine particles (Weidenschilling and Cuzzi 1993). Thus, this provides a natural way to separate particles by size. Another possibility is that if the nebula is turbulent, Cuzzi et al. (2001) showed that chondrule-sized particles can be locally concentrated by turbulent eddies. These eddies can locally increase the concentration of chondrule-sized particles but not particles of other sizes. More work is needed to investigate this possibility.

It should be remembered that the assumptions made in this model favored slow cooling rates for the particles. A more complex model, which accounts for three-dimensional radiative transfer and relaxation (cooling and expansion) of the gas in the relaxation zone, would likely predict more rapid cooling rates than those found here. If one imagines a cube radiating to space but only in one dimension (say, the x-direction), it will radiate energy at the rate of $2A_x\sigma T_4$, where A_x is the area of one cube face that is perpendicular to the x-axis, T is the temperature of the cube, σ is the Stefan-Boltzmann constant, and the factor of 2 is due to the second cube face that is perpendicular to the x-axis. If the cube is allowed to radiate energy away in all three directions it will lose energy at the rate of $2A_x\sigma T_4 + 2A_y\sigma T_4 + 2A_z\sigma T_4$, where A_y and A_z are the areas of the cube faces that are perpendicular to the y- and z-axes, respectively. Since a cube by definition has $A_x = A_y = A_z$, the total rate of energy loss would be $6A_x\sigma T_4$. Since we only consider a one-dimensional model, we likely are underestimating the cooling rates by a factor of ~ 3 , though the exact factor would depend on what the total volume (and dimensions) of the material processed by the bow shock was

(whether A_x differs greatly from A_y and A_z , for example). To fully determine the factor it would be necessary to determine the intensity of radiation in the other two dimensions (perpendicular to the initial gas velocity).

In addition, as shown in Fig. 3, the gas density in a bow shock begins to decrease immediately behind the shock front. As the density decreases, the number of collisions between the gas and the solids would also decrease. Once at rest with respect to the gas, the rate of heat input into a chondrule by thermal collisions with the gas is given by (Hood and Horanyi 1991):

$$\pi d^2 q = \rho_g (T_g - T_c) \left(\frac{\gamma + 1}{\gamma - 1} \right) \left(\frac{1}{8\sqrt{\pi}} \right) \left(\frac{2k}{m} \right)^{3/2} T_g^{1/2} \quad (22)$$

where ρ_g is the gas density, T_g is the temperature of the gas, T_c is the chondrule temperature, γ is the ratio of specific heat temperatures of the gas, m is the mean molecular mass of a nebular gas molecule, and k is Boltzmann's constant. Taking the typical values of these variables behind a shock wave once the chondrule has lost its relative velocity with respect to the gas ($\rho_g = 10^{-8}$ g/cm³, $T_g = 1600$ K, $T_c = 1500$ K, $\gamma = 1.4$, and $m = 4 \times 10^{-24}$ g), we find that the rate of heat input to the chondrule is $\sim 3 \times 10^5$ erg/s. If the gas density decreases by a factor of 10, as it does over a distance of ~ 5 planetesimal radii in these simulations, then q also decreases by a factor of 10 (making the generous assumption that the gas and chondrule temperatures remain the same), and thus the rate of heat input would decay to 3×10^4 erg/s. Assuming that the chondrule is 1.5×10^{-3} g and has a heat capacity of 10^7 erg/g/K, the loss of this heat input would correspond to an increase in cooling rate of ~ 18 K/s ($> 6 \times 10^4$ K/hr).

This increase in cooling rate would take place as the particle moved through the distance over which the gas density decreased. Looking at the case of a 1000 km planetesimal, this happens after a distance of ~ 5000 km. If the particle is moving at an average velocity (relative to the planetesimal) of 1 km/s (a typical speed in the post shock region), this means it takes the chondrule 5000 sec to traverse this distance. Thus, the cooling rate of the chondrule would increase by 0.0036 K/s/s or ~ 13 K/hr/s as the gas density decreases. Taking a conservative estimate that chondrules had to cool through a temperature range of just 50 K at a rate of 1000 K/hr or lower to form the textures and zoning observed in meteorites, this means that the chondrules would have to have cooled for a period of at least 0.05 hr or 180 sec. Over this time period, the cooling rate would have increased by 2300 K/hr using the numbers noted above. This again means that the cooling rates presented here likely are underestimates of the real cooling rates that particles would have experienced in the situations studied here. Thus, it is likely that even for the case in which the calculated cooling rates are within the expected range for chondrules, in a more realistic model, the cooling rates would be significantly higher than those presented here. The increase

would be most dramatic for smaller planetesimals as the expansion happens over a shorter distance.

While the treatments made in this model likely would lead to more rapid cooling, there are other effects that may help slow the cooling. If supersonic planetesimals existed during chondrule formation, then a large amount of solids could have been in the form of cm-sized bodies or larger, and most would be concentrated near the midplane of the nebula. If this is the location of planetesimal bow shocks, then it is possible that some of the m-sized bodies would also pass through these shocks along with chondrule precursors and fine-grained dust. These larger bodies would not be processed exactly like the smaller bodies, but they could transfer some of their kinetic energy into thermal energy of the gas as they speed through the shocked gas. This may help the gas maintain higher temperatures behind the shock front, which in turn would keep the chondrules from cooling too quickly. While this scenario cannot be ruled out, the efficiency and likelihood of such a scenario must be quantitatively investigated to maintain planetesimal bow shocks as a possible site of chondrule formation.

Finally, this work has not considered the shock wave that is created within 1.5 planetesimal radii of the planetesimal center. Along a trajectory that goes through the center of the planetesimal, the shock forms roughly 1 radius in front of the planetesimal's surface. Thus, for large planetesimals, this distance will be greater than the stopping distance of the chondrules (for planetesimals $>\sim 200$ km in radius). Chondrules could be heated and come to rest in front of the planetesimal without crashing into its surface. The chondrules, then, would likely be accelerated with the gas around the planetesimal. More work is needed to investigate how particles would cool if they entered a bow shock close to the planetesimal. However, this makes up a relatively small volume of the total shock that is formed, and thus may not be a very efficient mechanism. On the other hand, passing close to the planetesimal may make it easier for chondrules formed in this manner to be accreted into parent bodies. Future work will include a detailed investigation of this possibility.

Among the cases that we have considered, the larger planetesimals seem to be those that come closest to allowing silicates to be processed in a manner similar to how chondrules were processed. Planetesimals larger than 1000 km may still have been trapped in resonances with Jupiter and attained supersonic speeds (thus creating larger shock waves), but such objects would likely have been rare. Even if such objects did exist, the fraction of material in the asteroid belt region that they could process would be very small. For example, a 1000 km-radius planetesimal moving at 8 km/s would sweep out a volume (within 2 radii) on the order of 10^{23} cm³/s or 10^{37} cm³ during the few Myr that chondrules appear to have been produced. The volume of the asteroid belt region (2–4 AU) at low inclinations ($<1^\circ$) is $\sim 2 \times 10^{40}$ cm³. Thus, a body of this size would only process $\sim 0.1\%$ of the

solids. While multiple bodies may have existed (a few Earth masses would imply $\sim 10^3$ such bodies), only a few would be trapped at resonances at a given time, and those are the ones which would have velocities great enough to form shocks. Thus, only a few percent of the mass in the asteroid belt would be converted into chondrules. If chondritic meteorites represent the makeup of the majority of the asteroid belt, then this process seems to be too inefficient to explain the high volume of chondrules in primitive meteorites. If smaller planetesimals were capable of forming shocks which would form chondrules, the efficiency would increase (Weidenschilling et al. 1998). This becomes less of a problem if chondritic meteorites are not representative samples of the bulk asteroid belt.

Comparing the results of this work with those found in other studies (Desch and Connolly 2002; Ciesla and Hood 2002; Ciesla et al. 2003), we conclude that the thermal histories of particles in large scale shock waves (greater than a few 1000 km) more closely resemble those of chondrules than those in smaller scale shocks ($<\sim 1000$ km). Large shock waves are more efficient due to the large volumes of dense, hot gas and solids that are created. If the shocked gas does not decrease in density as quickly as shown in Fig. 3, then the decrease in heat input from the thermal collisions with the gas will not cause the chondrules to cool as quickly. Also, the large volume of hot, concentrated particles increases the intensity of radiation that particles are subject to, and thus helps them keep warm by allowing them to absorb more energy. If the gas properties began to rapidly relax back to their original state immediately behind the shock front in bow shocks (Fig. 3), this would cause the radiating solids to be less concentrated, which would decrease the heat input into the chondrules. This also means that if chondrule formation took place in a region of the nebula with a lower gas density than assumed here, the cooling rates would likely be too rapid to be consistent with chondrules, unless the shocks were significantly stronger and able to compress the gas by a greater amount.

Thus, if chondrules are a result of nebular shock waves, the shock waves could have been small in scale provided that they occurred in regions of the nebula with a low dust content to allow radiation from hot chondrules to travel great distances to keep the chondrules warm or must have been similar in scale to those predicted to be created by gravitational instabilities (Boss [2002] and earlier work by the same author) or due to the tidal interaction of Jupiter with the solar nebula (Bryden et al. 1999; Rafikov 2002). However, more work is needed to investigate whether these large shocks would occur in the proper region of the solar nebula to form chondrules, whether they were of the proper strength (velocity), and whether they can explain the ~ 2.5 -Myr age difference between CAIs and chondrules (Amelin et al. 2002). While they may not have been the main source of chondrules, supersonic planetesimals may still have been common in the solar nebula. Since the thermal processing predicted in planetesimal bow

shocks would be rapid (particularly for small planetesimals), these shocks may still have occurred without leaving any significant record in the chondrules (Jones et al. 2000). Whether or not the shocks could have left some other record in the meteorites remains to be investigated.

Acknowledgments—We thank Dante Lauretta, Jay Melosh, and Joshua Emery for insightful discussions. Reviews by Taishi Nakamoto, Patrick Cassen, and an anonymous reviewer resulted in significant improvements to this paper. This work was supported by a grant from NASA's Origins program.

Editorial Handling—Dr. David Mittlefehldt

REFERENCES

- Alibert Y., Mordasini C., and Benz W. 2004. Migration and giant planet formation. *Astronomy and Astrophysics* 417: L25–L28.
- Amelin Y., Krot A. N., Hutcheon I. D., and Ulyanov A. A. 2002. Lead isotopic ages of chondrules and calcium-aluminum-rich inclusions. *Science* 297:1678–1683.
- Boss A. P. 2002. Evolution of the solar nebula: V. Disk instabilities with varied thermodynamics. *The Astrophysical Journal* 576: 462–472.
- Bryden G., Chen X., Lin D. N. C., Nelson R. P., and Papaloizou J. C. B. 1999. Tidally induced gap formation in protostellar disks: Gap clearing and suppression of protoplanetary growth. *The Astrophysical Journal* 514:344–367.
- Chambers J. E. and Wetherill G. W. 2001. Planets in the asteroid belt. *Meteoritics & Planetary Science* 36:381–399.
- Ciesla F. J. and Hood L. L. 2002. The nebular shock wave model for chondrule formation: Shock processing in a particle-gas suspension. *Icarus* 158:281–293.
- Ciesla F. J., Lauretta D. S., Cohen B. A., and Hood L. L. 2003. A nebular origin for chondritic fine-grained phyllosilicates. *Science* 299:549–552.
- Colella P. and Woodward P. R. 1984. The piecewise parabolic method (PPM) for gas-dynamical simulations. *Journal of Computational Physics* 54:174–201.
- Connolly H. C. and Hewins R. H. 1995. Chondrules as products of dust collisions with totally molten droplets within a dust-rich nebular environment: An experimental investigation. *Geochimica et Cosmochimica Acta* 59:3231–3246.
- Cuzzi J. N., Hogan R. C., Paque J. M., and Dobrovolskis A. R. 2001. Size-selective concentration of chondrules and other small particles in protoplanetary nebula turbulence. *The Astrophysical Journal* 546:496–508.
- Cyr K. E., Sears W. D., and Lunine J. I. 1998. Distribution and evolution of water ice in the solar nebula: Implications for solar system body formation. *Icarus* 135:537–548.
- Desch S. J. and Connolly H. C. 2002. A model of the thermal processing of particles in solar nebula shocks: Application to the cooling rates of chondrules. *Meteoritics & Planetary Science* 37: 183–207.
- Hood L. L. 1998. Thermal processing of chondrule and CAI precursors in planetesimal bow shocks. *Meteoritics & Planetary Science* 33:97–107.
- Hood L. L. and Ciesla F. J. 2001. The scale size of chondrule formation regions: Constraints imposed by chondrule cooling rates. *Meteoritics & Planetary Science* 36:1571–1585.
- Hood L. L. and Horanyi M. 1991. Gas dynamic heating of chondrule precursor grains in the solar nebula. *Icarus* 93:259–269.
- Iida A., Nakamoto T., Susa H., and Nakagawa Y. 2001. A shock heating model for chondrule formation in a protoplanetary disk. *Icarus* 153:430–450.
- Jones R. H., Lee T., Connolly H. C., Love S. G., and Shang H. 2000. Formation of chondrules and CAIs: Theory versus observation. In *Protostars and planets IV*, edited by Mannings V., Boss A. P., and Russell S. S. Tucson: The University of Arizona Press. pp. 927–946.
- Marzari F. and Weidenschilling S. 2002. Mean motion resonances, gas drag, and supersonic planetesimals in the solar nebula. *Celestial Mechanics and Dynamical Astronomy* 82:225–242.
- Mayer L., Quinn T., Wadsley J., and Stadel J. 2002. Formation of giant planets by fragmentation of protoplanetary disks. *Science* 298:1756–1759.
- Miura H., Nakamoto T., and Susa H. 2002. A shock-wave heating model for chondrule formation: effects of evaporation and gas flows on silicate particles. *Icarus* 160:258–270.
- Moses J. I. 1992. Meteoroid ablation in Neptune's atmosphere. *Icarus* 99:368–383.
- Rafikov R. R. 2002. Planet migration and gap formation by tidally induced shocks. *The Astrophysical Journal* 572:566–579.
- Richards M. T. and Ratliff M. A. 1998. Hydrodynamic simulations of H alpha emission in Algol-type binaries. *The Astrophysical Journal* 493:326–342.
- Stevenson D. J. and Lunine J. I. 1988. Rapid formation of Jupiter by diffuse redistribution of water vapor in the solar nebula. *Icarus* 75:146–155.
- Wadhwa M. and Russell S. S. 2000. Timescales of accretion and differentiation in the early solar system: The meteoritic evidence. In *Protostars and planets IV*, edited by Mannings V., Boss A. P., and Russell S. S. Tucson: The University of Arizona Press. pp. 995–1018.
- Wasson J. T. 1996. Chondrule formation: Energetics and length scales. In *Chondrules and the protoplanetary disk*, edited by Hewins R. H., Jones R. H., and Scott E. R. D. Cambridge: Cambridge University Press. pp. 45–54.
- Wasson J. T. and Rubin A. E. 2003. Ubiquitous low-FeO relict grains in type II chondrules and limited overgrowths on phenocrysts following the final melting event. *Geochimica et Cosmochimica Acta* 67:2239–2250.
- Weidenschilling S. J. 1988. Formation processes and time scales for meteorite parent bodies. In *Meteorites and the early solar system*, edited by Kerridge J. F. and Matthews M. S. Tucson: The University of Arizona Press. pp. 348–371.
- Weidenschilling S. J. and Cuzzi J. N. 1993. Formation of planetesimals in the solar nebula. In *Protostars and planets III*, edited by Levy E. H. and Lunine J. I. Tucson: The University of Arizona Press. pp. 1031–1060.
- Weidenschilling S. J., Marzari F., and Hood L. L. 1998. The origin of chondrules at jovian resonances. *Science* 279:681–684.